



## Bubble confinement and deformation during flow boiling in microchannel<sup>☆</sup>



Liaofei Yin, Li Jia<sup>\*</sup>, Peng Guan

*Institute of Thermal Engineering, School of Mechanical, Electronic and Control Engineering, Beijing Jiaotong University, Beijing 100044, China  
Beijing Key Laboratory of Flow and Heat Transfer of Phase Changing in Micro and Small Scale, Beijing 100044, China*

### ARTICLE INFO

Available online 19 November 2015

#### Keywords:

Bubble confinement  
Wall confining force  
Flow boiling  
Microchannel

### ABSTRACT

The bubble dynamics during subcooled flow boiling were investigated in a single rectangular cross-section (0.5 mm × 1 mm) microchannel. Degassed deionized water was used as the working fluid with the confined bubble behavior observed using a high-speed CCD camera. The microchannel wall confines the bubble growth in the bubble height direction when the bubble departure diameter was larger than the microchannel cross section, resulting in strong deformation of the bubble top interface even before the liquid–vapor interface touched the microchannel wall. The microchannel confinement effect works by exerting a wall confining force on the top interface of the growing bubble. The negative feedback between the velocity of the top interface and the wall confining force is the main reason for the fluctuations in the increasing maximum local void fraction and the bubble aspect ratio during the confined bubble growth period.

© 2015 Elsevier Ltd. All rights reserved.

### 1. Introduction

Microchannel flow boiling has attracted much attention due to its high heat dissipation capability, which has great prospects for electronics cooling [1]. There has been much research on the mechanism for the high heat transfer efficiency of flow boiling in microchannels [2–4]. Many investigators believe that the microscale effects caused by the miniaturization of the dimensions create the outstanding heat transfer rates in microchannels [5,6]. Traditional viewpoints are that the large surface-to-volume ratio, negligible influence of the gravitational force and the higher ONB heat fluxes are the key microscale effects for flow boiling in microscale spaces. However, the bubble behavior in microscale boiling is quite different from that in conventional-scale systems. One of the most obvious differences is the occurrence of confined bubbles, which are regarded as the main reason for the enhanced heat dissipation capability in microscale systems [7,8]. Owing to the many promising applications of microbubbles in high-tech fields, like thermal ink jet printers [9], microfluidic chips [10], and thermal bubble actuated MEMS applications, some of researchers have paid more attention to understanding the bubble dynamics in microscale systems. Li and Cheng [11] investigated bubble nucleation during liquid flow in a microchannel. Deng et al. [12,13] observed the micro-bubble behavior on a platinum microheater with pulsed heating. Gedupudi et al. [14] studied the confined growth of bubbles during flow boiling in rectangular mini/micro-channels with two stages of partial and full confinement of single bubble growth. Wang and Sefiane [15] examined bubble

growth during flow boiling in high-aspect-ratio micro-channels, and presented a three-stage bubble growth model. They found that the evolution of bubble geometry is strongly related to the channel cross-sectional geometry, but is only slightly affected by the heat flux or mass flux. Yin et al. [16,17] studied bubble confinement and elongation during microchannel flow boiling by observing the formation of confined and elongated bubbles, and the force characteristics of the elongated bubble were analyzed theoretically.

Although some experiments have studied the unique bubble behavior at microscale, the details of bubble confined growth in microscale systems have not been fully understood. This paper describes an experimental investigation of bubble confinement in subcooled flow boiling in a microchannel to investigate the bubble deformation characteristics during confined growth. The effects of the heat flux, mass flux and inlet subcooling on the confined bubble growth are also studied.

### 2. Experimental setup

#### 2.1. Test loop configuration

The experimental system used to visualize the flow boiling in microchannels is shown schematically in Fig. 1. Deionized (DI) water was vigorously boiled to remove the non-condensable gases before being stored in the reservoir and then pumped into the test loop using a peristaltic pump. A 7 μm in-line micro-filter was used to remove any solid particles which may block the microchannel before the flow entered the test section. The pre-heater was used to adjust the inlet subcooling of the working fluid. The DI water in the microchannel test section was heated until a bubble nucleated on the channel wall. A

<sup>☆</sup> Communicated by W. J. Minkowycz.

<sup>\*</sup> Corresponding author.

E-mail address: [lja@bjtu.edu.cn](mailto:lja@bjtu.edu.cn) (L. Jia).

Nomenclature	
$g$	gravitational constant [ $\text{m/s}^2$ ]
$k$	empirical constant for bubble growth model
$n$	empirical constant for bubble growth model
$q_w$	heat flux [ $\text{W/m}^2$ ]
$t$	time [ms]
$Co$	confinement number
$D$	diameter [mm]
$G$	mass flux [ $\text{kg/m}^2 \text{ s}$ ]
$H$	height [mm]
$L$	length [mm]
$R$	bubble radius [mm]
$T$	temperature [K]
$W$	width [mm]
Greek	
$\alpha$	maximum local void fraction
$\beta$	bubble aspect ratio
$\rho$	density [ $\text{kg/m}^3$ ]
$\sigma$	surface tension [N/m]
Subscripts	
$b$	bubble
$c$	channel
$h$	hydraulic
$L$	liquid
$V$	vapor

high-speed CCD camera with micro-lens was used to visualize the bubble growth process. The liquid–vapor two-phase mixture exiting the test section flowed through a heat exchanger where the vapor phase was condensed. The working fluid was collected by a container placed on an electronic balance.

## 2.2. Test section

A single microchannel was milled into a thin copper plate. The cross section was rectangular with a width of 0.5 mm and a depth of 1 mm. The confinement number ( $Co = \sqrt{\sigma/g(\rho_L - \rho_V)D_h^2}$ ) of the channel was 3.9, indicating that the channel is a microchannel for flow boiling according to Kew and Cornwell [18]. The microchannel test piece was sandwiched between a polycarbonate cover plate and a Bakelite board with a sheet of Pyrex glass over the microchannel to protect the polycarbonate cover from thermal distortion as shown in Fig. 2. The heat flux was supplied by a ceramic heater glued to the back of the test piece.

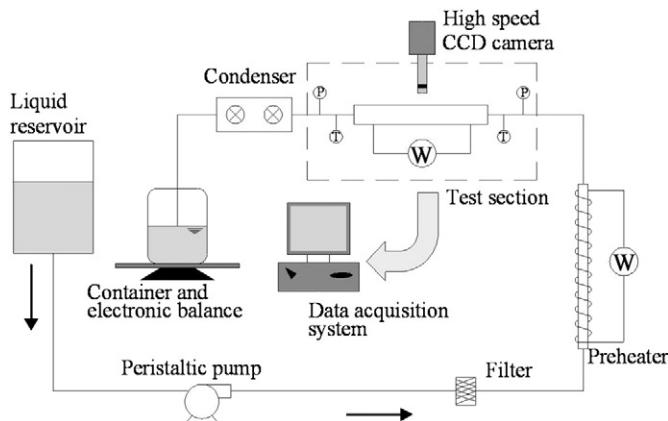


Fig. 1. Schematic diagram of the experimental apparatus.



Fig. 2. Schematic diagram of the test section.

Thermal insulation was wrapped around the test section to minimize heat losses to the ambient. The upper surface of the test section was exposed directly to the air, so the heat losses from this surface had to be subtracted to determine the net heat transfer between the working fluid and the microchannel wall [16]. Experiments were conducted at atmospheric pressure.

## 2.3. Measurements

The mass flow rate of the working fluid was determined by measuring the mass flow per unit time on a balance at the flow loop outlet. The working fluid temperatures at the test section inlet and outlet were measured by K-type thermocouples with accuracies of  $\pm 0.2$  °C. The machining precision of the microchannel was about  $\pm 0.02$  mm. The bubble dynamics were visualized by a high-speed CCD camera (USA, FASTEC IMAGING InLine 250) installed over the middle of the test section with the bubble dynamics recorded from the top at 250 frames per second (fps) with a spatial resolution of  $640 \times 478$  pixels. The object-to-image ratio of the recorded pictures was estimated as  $3.4 \mu\text{m}/\text{pixel}$ . The high-speed camera could record 8 s of video and the images were processed using the software MiDAS player. The bubble heights and lengths were determined by counting the pixels occupied by the bubble from its top to its bottom and between the upstream and downstream ends. The uncertainty in the bubble size measurements was about  $\pm 6.8 \mu\text{m}$  which a standard uncertainty analysis gave a maximum uncertainty of the maximum local bubble void fraction of  $\pm 12.8\%$  and of the bubble aspect ratio of  $\pm 15.2\%$ .

## 3. Results and discussion

A series of tests were conducted to observe the bubble confinement for various heat fluxes ( $q_w = 28.9 \text{ kW/m}^2$ – $69.2 \text{ kW/m}^2$ ) and inlet subcoolings ( $\Delta T_{\text{sub}} = 54$  °C– $77$  °C) at two mass fluxes ( $G = 33.3 \text{ kg/m}^2 \text{ s}$  and  $66.7 \text{ kg/m}^2 \text{ s}$ ).

### 3.1. Confined bubble growth

A complete bubble growth process recorded by the high-speed camera is shown in Fig. 3, where the top interface of the bubble near the confining wall deforms gradually from a spherical cap to a flat interface before the bubble top reaches the wall. The flattening of interface during the bubble top approaching the wall was similar with the bubble shape deformation during air bubble colliding with a rigid wall reported by Tsao et al. [19] and Malysa et al. [20], however, whose studying object was a moving air bubble in a water pool instead of the static and growing vapor bubble during flow boiling in microchannel. Therefore, it can be realized that the deformation feature of the bubble top interface during confined growth period is caused by the confining wall of the microchannel and is manifested as an additional pressure force which acts on the top interface of the bubble to deform the interface even before the top reaches the wall. In addition, this phenomenon of bubble shape deformation was observed in all tests in the present study, but has not been reported in the literature for flow boiling in conventional sized channels, thus it could be deduced that such bubble confinement only exists in microscale channels as a unique characteristic of microscale boiling.

Download English Version:

<https://daneshyari.com/en/article/652962>

Download Persian Version:

<https://daneshyari.com/article/652962>

[Daneshyari.com](https://daneshyari.com)